Modulating Efficiency and Stability of Methylammonium/Br-Free Perovskite Solar Cells Using Fluoroarene Hydrazine

Dhruba B. Khadka[1], Yasuhiro Shirai[1], Masatoshi Yanagida[1] and Kenjiro Miyano[1]

[1]Photovoltaics Materials Group, Global Research Center for Environment and Energy based on Nanomaterials Science (GREEN), National Institute for Materials Science (NIMS), 1-1 Namiki, Tsukuba, Ibaraki 305-0044, Japan

***Abstract* — Halide perovskite solar cells (PSCs) with state-of-the-art efficiencies consist of thermally unstable methylammonium (MA). In this report, we have employed the surface passivation method with multifunctional fluoroarene molecule, which suppresses the formation of PbI_2 and δ-perovskite phase in MA/Br-free perovskite film. The penta fluoro-phenylhydrazine (5F-PHZ) passivation effectively mitigates the defects at surface or grain boundaries in perovskite film with fluoroarene embedded interfacial layer as a consequence of stronger halogen bonding with fluoroarene moieties or $NH\text{-}NH_2$ terminal. As a result, the PSC with a p-i-n configuration achieved superior operational thermal stability and a PCE exceeding 22 % with a large area of ~1 cm^2. This work underscores a universal strategy for defect passivation to further improvement of efficiency using a multifunctional passivator. This report gives insights into the film growth properties, device photo-physics, and defect analysis correlating with device performance and device stability.**

I. Introduction

Lead perovskite solar cells (Pb-PSCs) have scaled up >25% benefiting from their exceptional optoelectronic properties. [1] However, this has imposed challenges for its practical application due to its lacking stability under heat and light stress as well as its susceptibility to a humid atmosphere. [2]–[7] The surface passivation approach has been widely employed in PSCs to improve the device parameters as well as stability. [8]

Several functional molecules have been used for passivating materials at the interfaces or additives in the perovskite precursor solution.[9]–[11] Gratzel and co-workers have used the fluoro in phenethyl chain as passivating materials for the improvement in device performance and its stability under a higher humid atmosphere.[12] Therefore, it is of great interest to explore the fluorinated functional materials in PSCs for modulating device performance and stability.

Here, we introduced a fluoroarene-anchored functional material; penta fluoro-phenylhydrazine (5F-PHZ) for interface treatment onto the MA-free Pb-HaP. This approach enhanced the device performance as high as 22.29 % (A~1 cm^2) with superior operational stability. The 5F-PHZ treatment has shown a significant impact on the morphology, interface chemistry, and optoelectronic properties of HaP films. This report has discussed the synergetic effect in film growth and photo-physics of PSCs with interfacial passivation.

II. EXPERIMENTAL

A. Device fabrication

For the fabrication of MA-free RB-HaP; $FA_{0.84}Cs_{0.12}Rb_{0.04}PbI_3$: the precursor solution (1.05 M) was prepared by dissolving FAI (0.84 M), CsI (0.12 M), RbI (0.04 M), PbI_2 (1 M), and 5-AVAI (1 mM) in the mixture of dimethylformamide and dimethyl sulfoxide (4:1) solvent for 2 hours. The sputtered NiO_x thin film was treated with MeO-2PACz by spin coating at 5000 rpm -50 s and subsequently dried at 100 ℃ for 10 min. For film deposition, the precursor was spin-coated at 1000 rpm-10 s and 5000 rpm-40 s followed by dripping 800 µl of CB at 34^{th} s of 2^{nd} step. Then, these as-grown films were simply placed on a hot plate at 60℃ for 1 min and at 100℃ for 45 min. For surface passivation, 5F-PHZ precursor solutions of different concentration (0.5 - 10 mol%/ml) was spin-coated onto the HaP film at 5000 rpm-40 s and annealed at 100℃-5 min. Then, we deposited C_{60} and BCP by thermal evaporation. Finally, Ag was thermally evaporated and get device. The detailed fabrication can be found in our earlier reports.[13], [14]

B. Materials and device characterizations

XRD patterns were measured using Rigaku Smart Lab, CuKα radiation, λ=1.5405Å. Scanning electron microscopy (SEM) images were obtained by a high-resolution scanning electron microscope (SEM) at 5 kV accelerating voltage (Hitachi, S-4800). The absorption and photoluminescence (PL) spectra were measured using UV-Vis-NIR spectrometer (UV-2600i, Shimadzu) and micro-PL spectrometer (HORIBA, LabRamHR-PL NF(UV-NIR). The current density–voltage (J-V) curves were measured under 1 sun with an AM1.5G spectral filter coupled with an MPPT system (Systemhouse Sunrise Corp.). Device certification was conducted in the National Institute of Advanced Industrial Science and Technology (AIST), Japan. It is registered as ISO / IEC 17025 accreditation laboratory (IA Japan ASNITE 0021 Calibration) according to international mutual recognition arrangements (MRA) for international laboratory (ILAC), and Asia pacific accreditation cooperation (APAC). Capacitance spectra (C–f) were collected using an LCR meter (IM3536, Hioki) under dark.

III. RESULTS AND DISCUSSION

To examine the photovoltaic effect of 5F-PHZ treatment, the device structure is as depicted in Fig. 1a. The 5F-PHZ molecule is shown in the adjoining figure.

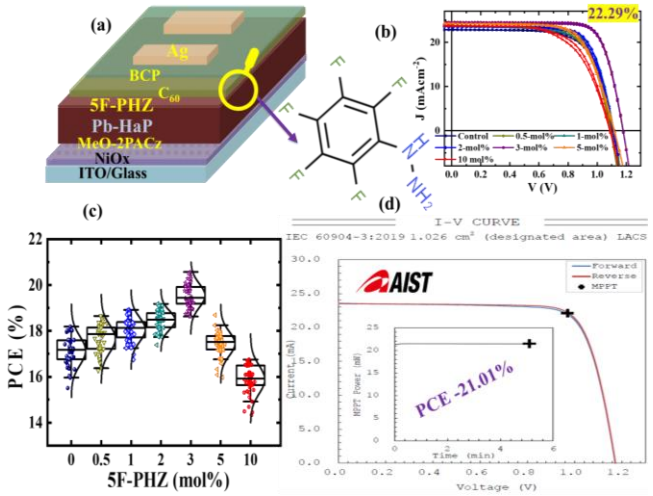

Figure 1. Device structure and molecular structure of 5F-PHZ (a). The J-V curves of Pb-PSCs with 5F-PHZ treatment concentartions (for x=0 – 10 mol%) (b). Device efficiency trend (c) and certified device efficiency (device of area 1.026 cm^2, at AIST).

Figure 1b presents the current density-voltage (J-V) curves of the control and 5F-PHZ passivation device with varying concentrations. The control device yields a PCE of 18.10%. The 5F-PHZ (3 mol%) treated device achieved PCE of 22.29% with an increase in V_{OC} ~ 1.096 to 1.178 V, J_{SC} ~ 22.88 to 24.51 $mAcm^{-2}$, and FF ~72.2 to 77.2%. The J-V curve with 5F-PHZ treated device has negligible hysteresis. It is reported that the fluorinated aromatic rings and NH-NH_2 terminals interact with perovskite and hence minimize the iodine vacancy, surface defect, and its migration with strong halogen bonding.[12] The PCE statistics as a function of the 5F-PHZ concentration is depicted in Figure 1c. The device efficiency was certified with PCE of ~21.01% (~1.026 cm^2) in accredited independent photovoltaic test laboratory (AIST PV Lab, Japan) (Fig. 1d).

Figures 2a-c show SEM images of Pb-HaP with 5F-PHZ treatment. It indicates the film formation with a slight increase in grain size with a faint indication of the formation of an overlayer on the perovskite grain domain. A HaP Film with a higher concentration grows with overlayer surface features as a consequence of the adsorption of 5F-PHZ forming a 2D phase interacting with the lead iodide.

XRD patterns (Fig. 2d) were collected to investigate crystal growth. The control film grows with the dominant (110) plane of α-phase of HaP along with weak peaks of the δ- phase and residual PbI_2. Importantly, the characteristic diffraction peaks of δ- phase and PbI_2 disappeared on the 5F-PHZ treated (~3 mol%) indicating the growth of better film quality. While an additional XRD peak appeared at <10° in the film 5F-PHZ (≥10 mol%) suggesting the formation of a 2D phase of $(5F\text{-}PHZ)_2PbI_4$.This observation underlines the importance of the 5F-PHZ treatment from the surface for improving perovskite film quality.

Figure 2. Effect of 5F-PHZ treatment: SEM image (a-c)), XRD

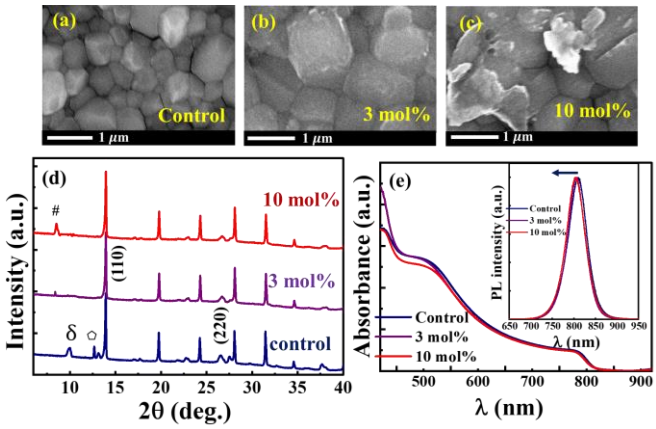

patterns (#-2D phase, δ- non-photoactive perovskite phase, ⬠-PbI_2) (d), absorption spectra (e) (Inset- PL spectra).

The UV-vis spectra (Figure 2e) of respective films indicate no notable effect on absorption spectra of HaP films. The PL spectra (Fig. inset) also do not show any notable feature except a slight blue shift of PL characteristic peak (~819 to 817 nm).

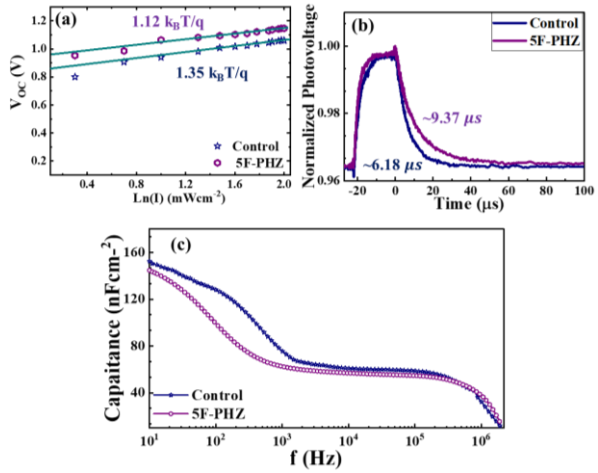

Fig. 3. Device characteristics; V_{OC}-I plot (a), TPV spectra (b), C-f spectra at room temperature (c).

To gain insight into photophysics, we investigated the light-intensity-dependent V_{OC} (Fig. 3a). The control device reveals a slope of 1.35 kBT/q which is higher than the 5F-PHZ treated device (1.12 kBT/q) indicating a reduction in trap-assisted recombination.[15], [16]

Figure 3b depicts the transient photovoltage (TPV) under transient illumination. The TPV decay signals demonstrates a carrier lifetime of 6.18 μs for the control device which is longer for the 5F-PHZ treated device (9.37 μs), indicating well consistency with device performance dut to defect passivation.

Moreover, Figure 3c depicts the capacitance-frequency (C-f) spectra under the dark showing a slightly higher value in the plateau regime (1 to 100 kHz) that stems from the HaP layer accounting for defect dynamics. While the capacitance at a lower frequency reveals a much steeper feature for the control device. Thus, it indicates suppression of interfacial charge accumulation for the device with 5F-PHZ treatment.

IV. SUMMARY AND CONCLUSIONS

We demonstrated interfacial passivation on 3D-HaP to modulate the efficiency and stability of the inverted PSCs with sputtered NiO_x as HTL, enhanced PCE from ~18.10 to 22.29%. This surface treatment with 5F-PHz significantly modifies the surface chemistry and interfacial energy band due to strong halogen bonding induced by fluoroarene moieties coated on a 3D surface. The device analysis corroborates the suppression of defect densities for the 5F-PHZ treated device due to halogen bonding interaction with various fluoroarene derivatives.

ACKNOWLEDGMENT

This work was supported by JST-Mirai Program Grant Number JPMJMI21E6, Japan.

REFERENCES

[1] O. Almora *et al.*, "Device Performance of Emerging Photovoltaic Materials (Version 3)," *Adv. Energy Mater.*, vol. 13, no. 1, p. 2203313, Jan. 2023, doi: 10.1002/aenm.202203313.

[2] W. Tress *et al.*, "Performance of perovskite solar cells under simulated temperature-illumination real-world operating conditions," *Nat. Energy*, vol. 4, no. 7, pp. 568–574, 2019, doi: 10.1038/s41560-019-0400-8.

[3] D. B. Khadka, Y. Shirai, M. Yanagida, and K. Miyano, "Insights into Accelerated Degradation of Perovskite Solar Cells under Continuous Illumination Driven by Thermal Stress and Interfacial Junction," *ACS Appl. Energy Mater.*, vol. 4, no. 10, pp. 11121–11132, Oct. 2021, doi: 10.1021/acsaem.1c02037.

[4] D. B. Khadka, Y. Shirai, M. Yanagida, and K. Miyano, "Degradation of encapsulated perovskite solar cells driven by deep trap states and interfacial deterioration," *J. Mater. Chem. C*, vol. 6, no. 1, pp. 162–170, 2018, doi: 10.1039/C7TC03733C.

[5] I. Gueye *et al.*, "Chemical and Electronic Investigation of Buried NiO 1−δ,PCBM, and PTAA/MAPbI3–xClx Interfaces Using Hard X-ray Photoelectron Spectroscopy and Transmission Electron Microscopy," *ACS Appl. Mater. Interfaces*, vol. 13, no. 42, pp. 50481–50490, 2021, doi: 10.1021/acsami.1c11215.

[6] D. B. Khadka, Y. Shirai, M. Yanagida, K. Uto, and K. Miyano, "Analysis of degradation kinetics of halide perovskite solar cells induced by light and heat stress," *Sol. Energy Mater. Sol. Cells*, vol. 246, p. 111899, Oct. 2022, doi: 10.1016/j.solmat.2022.111899.

[7] I. Gueye *et al.*, "Analysis of Iodide Transport on Methyl Ammonium Lead Iodide Perovskite Solar Cell Structure Through Operando Hard X-ray Photoelectron Spectroscopy," *Chem. Mater.*, vol. 35, no. 5, pp. 1948–1960, Mar. 2023, doi: 10.1021/acs.chemmater.2c03162.

[8] Y. Liu *et al.*, "Ultrahydrophobic 3D/2D fluoroarene bilayer-based water-resistant perovskite solar cells with efficiencies exceeding 22%," *Sci. Adv.*, vol. 5, no. 6, p. eaaw2543, Jun. 2019, doi: 10.1126/sciadv.aaw2543.

[9] A. Q. Alanazi *et al.*, "Atomic-Level Microstructure of Efficient Formamidinium-Based Perovskite Solar Cells Stabilized by 5-Ammonium Valeric Acid Iodide Revealed by Multinuclear and Two-Dimensional Solid-State NMR," *J. Am. Chem. Soc.*, vol. 141, no. 44, pp. 17659–17669, 2019, doi: 10.1021/jacs.9b07381.

[10] D. B. Khadka, Y. Shirai, M. Yanagida, and K. Miyano, "Pseudohalide Functional Additives in Tin Halide Perovskite for Efficient and Stable Pb-Free Perovskite Solar Cells," *ACS Appl. Energy Mater.*, vol. 4, no. 11, pp. 12819–12826, Nov. 2021, doi: 10.1021/acsaem.1c02496.

[11] Z. Wang *et al.*, "Efficient ambient-air-stable solar cells with 2D–3D heterostructured butylammonium-caesium-formamidinium lead halide perovskites," *Nat. Energy*, vol. 2, no. 9, p. 17135, Aug. 2017, doi: 10.1038/nenergy.2017.135.

[12] M. A. Ruiz-Preciado *et al.*, "Supramolecular Modulation of Hybrid Perovskite Solar Cells via Bifunctional Halogen Bonding Revealed by Two-Dimensional 19 F Solid-State NMR Spectroscopy," *J. Am. Chem. Soc.*, vol. 142, no. 3, pp. 1645–1654, Jan. 2020, doi: 10.1021/jacs.9b13701.

[13] D. B. Khadka, Y. Shirai, M. Yanagida, T. Tadano, and K. Miyano, "Interfacial Embedding for High-Efficiency and Stable Methylammonium-Free Perovskite Solar Cells with Fluoroarene Hydrazine," *Adv. Energy Mater.*, vol. 12, no. 38, p. 2202029, Oct. 2022, doi: 10.1002/aenm.202202029.

[14] D. B. Khadka, Y. Shirai, M. Yanagida, and K. Miyano, "Unraveling the Impacts Induced by Organic and Inorganic Hole Transport Layers in Inverted Halide Perovskite Solar Cells," *ACS Appl. Mater. Interfaces*, vol. 11, no. 7, pp. 7055–7065, Feb. 2019, doi: 10.1021/acsami.8b20924.

[15] D. B. Khadka *et a*l., "Enhancement in efficiency and optoelectronic quality of perovskite thin films annealed in MACl vapor," *Sustain. Energy Fuels*, vol. 1, no. 4, pp. 755–766, 2017, doi: 10.1039/C7SE00033B.

[16] D. B. Khadka, Y. Shirai, M. Yanagida, and K. Miyano, "Ammoniated aqueous precursor ink processed copper iodide as hole transport layer for inverted planar perovskite solar cells," *Sol. Energy Mater. Sol. Cells*, vol. 210, p. 110486, 2020, doi: https://doi.org/10.1016/j.solmat.2020.110486.